The host scaffolding protein Filamin A and the exocyst complex control exocytosis during InlB-mediated entry of *Listeria monocytogenes*

Manmeet Bhalla[a], Hoan Van Ngo[a,b], Gaurav Chandra Gyanwali[a], and Keith Ireton[a,*]

[a] Department of Microbiology and Immunology, University of Otago, Dunedin, New Zealand

[b] Present address: Department of Immunology and Infection, Faculty of Infectious and Tropical Diseases, London School of Hygiene and Tropical Medicine, London, United Kingdom.

* Address correspondence to Keith Ireton, keith.ireton@otago.ac.nz.

Running title:

Control of host exocytosis during InlB-mediated entry

SUMMARY

Listeria monocytogenes is a food-borne bacterium that causes gastroenteritis, meningitis, or abortion. *Listeria* induces its internalization (entry) into some human cells through interaction of the bacterial surface protein InlB with its host receptor, the Met tyrosine kinase. InlB and Met promote entry, in part, through stimulation of localized exocytosis. How exocytosis is upregulated during entry is not understood. Here we show that the human signaling proteins mTOR, Protein Kinase C (PKC)-α, and RalA promote exocytosis during entry by controlling the scaffolding protein Filamin A (FlnA). InlB-mediated uptake was accompanied by PKC-α –dependent phosphorylation of serine 2152 in FlnA. Depletion of FlnA by RNA interference (RNAi) or expression of a mutated FlnA protein defective in phosphorylation impaired InlB-dependent internalization. These findings indicate that phosphorylation of FlnA by PKC-α contributes to entry. mTOR and RalA were found to mediate the recruitment of FlnA to sites of InlB-mediated entry. Depletion of PKC-α, mTOR, or FlnA each reduced exocytosis during InlB-mediated uptake. Because the exocyst complex is known to mediate polarized exocytosis, we examined if PKC-α, mTOR, RalA, or FlnA affect this complex. Depletion of PKC-α, mTOR, RalA, or FlnA impaired recruitment of the exocyst component Exo70 to sites of InlB-mediated entry. Experiments involving knockdown of Exo70 or other exocyst proteins demonstrated an important role for the exocyst complex in uptake of *Listeria*. Collectively, our results indicate that PKC-α, mTOR, RalA, and FlnA comprise a signaling pathway that mobilizes the exocyst complex to promote infection by *Listeria*.

INTRODUCTION

Listeria monocytogenes is a food-borne bacterium that causes gastroenteritis, meningitis or abortion (1). Critical for disease is the ability of *Listeria* to induce its internalization (entry) into nonphagocytic cells in the intestine, liver, or placenta (2). A major pathway of *Listeria* entry is mediated by binding of the bacterial surface protein InlB to its host receptor, the Met tyrosine kinase (3). Binding of InlB activates Met, resulting in the stimulation of two host processes that promote bacterial uptake: actin polymerization and exocytosis (4-6).

Actin polymerization is thought to contribute to entry of *Listeria* by providing a protrusive force that drives the host plasma membrane around adherent bacteria (4, 7). Exocytosis is the fusion of intracellular vesicles with the plasma membrane (8). How membrane flow through exocytosis controls InlB-dependent uptake is not fully understood. One potential mechanism involves the delivery of the GTPase Dynamin 2 to the host plasma membrane (6). During InlB-mediated entry, Dynamin 2 translocates from an internal membrane compartment termed the recycling endosome (RE) to sites in the plasmalemma near adherent bacteria. Dynamin 2 is known to remodel membranes through a GTP-dependent scission activity and also through interaction with membrane sculpting proteins containing BAR domains (9). These membrane remodeling activities of Dynamin 2 are likely responsible for its role in InlB-mediated entry (6, 10).

How are actin polymerization and exocytosis stimulated during InlB-dependent uptake of *Listeria*? Substantial progress has been made on the mechanism of actin polymerization, revealing that this process is mediated by the host Arp2/3 complex and the nucleation promoting factors N-WASP and WAVE (5, 11, 12). By contrast, little is known about how exocytosis is induced during InlB-mediated

internalization, except that induction requires the kinase activity of Met and the host GTPase RalA (6).

Previous results demonstrated that the human serine/threonine kinases mTOR and Protein Kinase C-α (PKC-α) are activated downstream of Met and play important roles in InlB-mediated entry of *Listeria* (13). mTOR and PKC-α comprise a signaling pathway involved in several biological events, including cell migration and survival (14, 15). mTOR forms part of a multi-component complex called mTORC2 that phosphorylates serine 657 in a hydrophobic motif in PKC-α, thereby upregulating PKC kinase activity (16). Importantly, InlB-mediated entry of *Listeria* is accompanied by mTOR-dependent phosphorylation of serine 657 in PKC-α, indicating that mTOR functions upstream of PKC-α during entry (13). How mTOR and PKC-α control internalization of *Listeria* is not well understood. Although PKC-α has a minor role in actin polymerization during entry, mTOR has no detectable effect on this process (13). It therefore seems likely that mTOR and PKC-α affect uptake of *Listeria* by regulating host processes apart from the assembly of actin filaments. One such process could be exocytosis.

In this work, we show that mTOR and PKC-α promote exocytosis during InlB-mediated entry of *Listeria* by controlling the human scaffolding protein Filamin A (FlnA). InlB-dependent internalization was accompanied by an increase in phosphorylation of serine 2152 in FlnA, an event mediated by PKC-α. mTOR promoted recruitment of FlnA to sites of InlB-mediated entry. The GTPase RalA was also needed for FlnA recruitment. Depletion of FlnA by RNA interference (RNAi) or expression of a mutated form of FlnA that is not phosphorylated on serine 2152 inhibited entry, indicating an important role for FlnA in infection by *Listeria*. Further experiments revealed that mTOR, PKC-α, and RalA each control exocytosis during

entry by recruiting the exocyst, a multicomponent complex known to promote exocytosis by tethering vesicles to sites in the plasma membrane (17). RNAi experiments demonstrated an important role for the exocyst complex in InlB-mediated entry. Collectively, these findings identify a host signaling pathway that controls the exocyst complex to promote infection of human cells by *Listeria*.

RESULTS

The host scaffolding protein FlnA promotes InlB-mediated entry of *Listeria*

Previous results demonstrated that the host serine/threonine kinases mTOR and PKC-α act together to control InlB-mediated entry of *Listeria* (13). In order to better understand how these two kinases regulate InlB-dependent internalization, we focused our attention on FlnA, a protein that bundles actin filaments and assembles multi-molecular signaling complexes (18). This protein is known to interact with PKC-α or the mTORC2 component Rictor, and is directly phosphorylated by PKC-α (19-22).

We used RNAi to examine the role of FlnA in InlB-mediated invasion of *Listeria* into the human epithelial cell line HeLa. In order to control for potential off-target effects (23), three different siRNAs targeting distinct sequences in FlnA mRNA were used. Control conditions included mock transfection in the absence of siRNA or transfection with a control "non-targeting" siRNA that lacks complementarity to any known mRNA. Importantly, each of the three siRNAs against FlnA reduced expression of the target protein and inhibited invasion of *Listeria* into HeLa cells compared to the control conditions (Fig. 1A,B).

We also determined the effect of siRNA-mediated depletion of FlnA on entry of inert particles coated with InlB. Latex beads (3 μm in diameter) have been extensively used as a model for InlB-dependent entry, since these particles lack other bacterial factors and are efficiently internalized into mammalian cells in a manner that depends on the Met receptor and other host proteins involved in *Listeria* uptake (6, 11-13, 24-28). As previously reported (6, 13, 26, 29), beads coupled to InlB were efficiently internalized into HeLa cells, whereas control beads coupled to glutathione S-transferase (GST), were not internalized (Fig. 1Ci). Next, the siRNA against FlnA

123 that caused the largest inhibition in invasion of *Listeria* was used to deplete FlnA in
124 HeLa cells and the effect on uptake of InlB-coated beads was assessed. Internalization
125 of beads was inhibited by about 40% (Fig. 1Cii). Taken together, the results in Figure
126 1 indicate an important role for host FlnA in InlB-dependent entry.
127
128 **InlB induces PKC-α -dependent phosphorylation of FlnA**
129 FlnA is comprised of an amino-terminal actin binding domain and 24
130 immunoglobulin (Ig)-like domains (18). One of the phosphorylation sites for FlnA is
131 serine 2152, located in Ig domain 20. Phosphorylation of this residue controls several
132 biological events, including focal adhesion formation, lamellipodia formation, protein
133 trafficking, and cell migration (20, 22, 30-33).
134 We investigated whether the InlB-mediated pathway of entry involves
135 phosphorylation of serine 2152 in FlnA. The effects of InlB on FlnA phosphorylation
136 were assessed in two different conditions: treatment of mammalian cells with soluble
137 InlB protein and entry of InlB-coated beads. When used at low nanomolar
138 concentrations, soluble InlB is a potent agonist of the Met receptor and its associated
139 downstream signaling pathways (3, 13, 34, 35). Importantly, treatment of HeLa cells
140 with 4.5 nM of soluble InlB for 10 min caused an increase in reactivity of cell lysates
141 with antibodies generated against phosphorylated serine 2152 in FlnA (Fig. 2Ai).
142 Results from two types of control experiments indicated that these anti-phospho-FlnA
143 antibodies recognize predominantly phosphorylated serine 2152 in FlnA in HeLa
144 cells. First, transfection of HeLa cells with an siRNA targeting FlnA reduced
145 reactivity with the anti-phospho-FlnA antibodies (Fig. 2Ai). Secondly, substitution of
146 serine 2152 with an alanine residue (S2152A) decreased reactivity with these

antibodies (Fig. 2Aii). Collectively, the results in Figure 2A indicate that soluble InlB stimulates phosphorylation of serine 2152 in FlnA.

Several serine/threonine kinases including PAK1, p70S6K, and PKC-α are known to phosphorylate S2152 in FlnA (19 20, 30, 36). Since PKC-α plays an important role in InlB-mediated entry of *Listeria* (13), we examined if this kinase mediates phosphorylation of FlnA induced by InlB. Importantly, siRNA-mediated depletion of PKC-α reduced phosphorylation of FlnA on serine 2152 in HeLa cells treated with soluble InlB protein (Fig. 2B). The Met receptor is required for InlB-induced activation (phosphorylation) of PKC-α (13). As expected, siRNA-mediated knockdown of Met inhibited FlnA phosphorylation of serine 2152 (Fig. 2C). These results demonstrate that Met and PKC-α are needed for efficient phosphorylation of FlnA in response to InlB.

Experiments involving InlB-coated beads demonstrated that incubation with these particles stimulated phosphorylation of FlnA on serine 2152 (Figure 2D). These findings demonstrate that phosphorylation of FlnA increases during InlB-mediated entry.

Phosphorylation of FlnA contributes to InlB-mediated entry

In order to determine if phosphorylation of FlnA on serine 2152 affects InlB-dependent internalization, we used a FlnA mutant protein containing a serine-to-alanine substitution at amino acid 2152. This S2152A mutation in FlnA causes defects in membrane ruffling (30), cell migration (32), or trafficking of the lipid raft component caveolin-1 (20), indicating that it perturbs FlnA function. We compared the efficiency of InlB-mediated entry into HeLa cells transiently expressing myc-tagged wild-type FlnA or FlnA.S2152A. The myc-FlnA wild-type and myc-

FlnA.S2152A proteins were expressed at similar levels, as assessed by Western blotting (Figure 3A) or confocal microscopy analysis (Fig. 3Bii). Importantly, entry of InlB-coated beads was about 35% lower into cells expressing myc-FlnA.S2152A compared to cells expressing the myc-FlnA wild-type protein (Fig. 3Bi). These results indicate that phosphorylation of FlnA on serine 2152 contributes to InlB-dependent uptake.

mTOR and RalA mediate recruitment of FlnA during InlB-dependent entry

Incubation of HeLa cells with InlB-coated beads resulted in accumulation of FlnA in cup-like structures around particles (Fig. 4A). By contrast, incubation with control GST-coated beads failed to induce FlnA accumulation. Accumulation of FlnA was quantified by measuring fold enrichment (FE) values, essentially as described (6, 13, 28, 29). FE is defined as the mean fluorescence intensity of a host protein of interest in a cup-like structure around beads normalized to the mean fluorescence intensity of the protein throughout the entire human cell. An FE value greater than 1.0 indicates enrichment of the host protein around particles. The mean FE value for FlnA in control conditions involving HeLa cells that were mock transfected or transfected with control siRNA was about 1.35, indicating enrichment (Figure 4B). By comparison, the mean FE value for cells incubated with GST-coated beads was less than 1.0. These results demonstrate that InlB induces a redistribution of FlnA, causing this host protein to accumulate at sites of particle internalization.

We next examined the roles of mTOR, PKC-α, and Met in recruitment of FlnA during entry. We previously reported that siRNAs targeting mTOR, PKC-α, or Met inhibit entry of InlB-coated beads into HeLa cells (6, 13). Using these same

siRNAs, we found that RNAi against mTOR or Met, but not PKC-α, impaired accumulation of FlnA around InlB-coated beads (Figure 4).

FlnA is known to interact with the activated form of the GTPase RalA, and this interaction recruits FlnA to filopodia (37). We previously reported that RalA is needed for efficient entry of *Listeria* and InlB-coated beads into HeLa cells (6). Here we found that siRNA-mediated depletion of RalA prevented accumulation of FlnA around InlB-coated beads (Fig. 4). These results suggest that RalA may control InlB-dependent internalization, in part, through recruitment of FlnA. Taken together, the results in Figures 4 indicate that mTOR and RalA act upstream of FlnA to localize this protein to sites of InlB-mediated entry.

mTOR, PKC-α, and FlnA control exocytosis during InlB-mediated entry

RNAi-based studies indicate that localized exocytosis during InlB-dependent entry requires the Met receptor and RalA (6). Since RalA controls recruitment of FlnA (Fig. 4), we tested the possibility that FlnA and its regulators mTOR and PKC-α might promote exocytosis during InlB-mediated entry. Exocytosis was detected using a probe consisting of the v-SNARE protein VAMP3 fused to GFP (6, 38). Prior to exocytosis, VAMP3-GFP resides in intracellular vesicles. When vesicles fuse with the plasma membrane during exocytosis, the GFP moiety becomes extracellular (exofacial) and can be labeled with antibodies without cell permeabilization.

HeLa cells were subjected to control conditions or transfected with siRNAs against mTOR, PKC-α, FlnA, or Met. As a negative control for a condition previously found to not affect exocytosis, HeLa cells were transfected with an siRNA targeting the Arp3 component of the Arp2/3 complex (6, 29). After siRNA transfection, cells were transfected with a plasmid expressing VAMP3-GFP,

incubated with beads coated with InlB or GST, fixed, and labeled for exofacial VAMP3-GFP as described (6, 38). Images were acquired by confocal microscopy, and exocytosis was quantified as FE values for exofacial VAMP3-GFP, as described (6). The results indicate that siRNAs against mTOR, PKC-α, FlnA, or Met each reduced exocytosis around InlB-coated particles (Fig. 5). By contrast, the siRNA targeting Arp3 did not affect exocytosis around beads, consistent with previous findings (6). Importantly, experiments in this study or in previously published work indicate that each of the siRNAs used against mTOR, PKC-α, FlnA, Met, or Arp3 inhibit target protein expression and internalization of InlB-coated beads (Fig. 1A,C) (6, 13, 26, 29). Taken together, the findings in Figure 5 demonstrate important functions for mTOR, PKC-α, and FlnA in exocytosis during InlB-dependent internalization.

Given the role of FlnA in exocytosis during entry, we next determined if phosphorylation of S2152 affects this host process. HeLa cells were co-transfected with plasmids expressing the exocytic probe VAMP3-GFP and myc-tagged wild-type FlnA or FlnA.S2152A. After acquisition of images using confocal microscopy, the degree of exocytosis in cells expressing either myc-tagged FlnA protein was quantified as FE values for exofacial VAMP3-GFP. The results, presented in Figure 6, show that exocytosis was ~ 40% lower in cells expressing myc-FlnA.S2152A compared to in cells expressing wild-type FlnA. These findings indicate that phosphorylation of serine 2152 contributes to exocytosis during InlB-mediated entry.

mTOR, PKC-α, RalA, and FlnA control exocytosis by recruiting the exocyst complex

RalA is known to stimulate exocytosis through the exocyst complex (17, 39). This complex is comprised of eight proteins (Sec3, Sec5, Sec6, Sec8, Sec10, Sec15, Exo70, and Exo84) and tethers vesicles to the plasma membrane in a step preceding fusion of these vesicles with the plasma membrane. RNAi studies indicated roles for the exocyst components Sec3, Sec5, Sec8, and Exo70 in invasion of *Listeria* or entry of InlB-coated beads into HeLa cells (Figures 7 and S1).

Experiments with constructs comprised of Exo70, Sec5, Sec8, or Sec15 fused to GFP demonstrated that these host proteins accumulate around InlB-coated beads during particle entry (Fig. S2A). Immunolabeling of endogenous Exo70, Sec5, or Sec8 also indicated recruitment (Fig. S2B). Of all the endogenous or GFP-tagged proteins examined, GFP-Exo70 displayed the most pronounced accumulation around InlB-coated beads. We therefore assessed the roles of mTOR, PKC-α, RalA, and FlnA in GFP-Exo70 recruitment. Importantly, treatment of HeLa cells with siRNAs against mTOR, PKC-α, or FlnA each reduced accumulation of GFP-Exo70 around InlB-coated beads (Fig. 8). An siRNA targeting Arp3 did not affect accumulation of GFP-Exo70 around InlB-coated beads, consistent with the lack of effect of Arp3 RNAi on exocytosis (Fig. 8) (6). Collectively, these results demonstrate that mTOR, PKC-α, RalA, and FlnA mobilize Exo70 to plasma membrane sites during particle internalization.

Further experiments demonstrated that the exocyst complex mediates exocytosis during InlB-dependent entry. RNAi-mediated depletion of Sec3, Sec5, Sec8, or Exo70 each reduced the accumulation of exofacial VAMP3-GFP that normally occurs around InlB-coated particles (Fig. 9). Taken together, the results in Figures 8 and 9 demonstrate that mTOR, PKC-α, RalA, and FlnA control recruitment of the exocyst complex to promote exocytosis during InlB-dependent uptake.

DISCUSSION

In this study, we demonstrated that host mTOR, PKC-α, and FlnA each promote exocytosis during InlB-mediated entry of *Listeria*. Our previous results indicate that the host GTPase RalA also contributes to exocytosis during entry (6). The findings in this work, combined with the previous results with RalA, suggest that mTOR, PKC-α, RalA, and FlnA form a signaling pathway that controls exocytosis through recruitment of Exo70, a component of the exocyst complex. Evidence for such a pathway is that PKC-α is needed for efficient phosphorylation of FlnA on serine 2152, and that both mTOR and RalA mediate the recruitment of FlnA to sites of InlB-mediated uptake. Collectively, these results suggest that FlnA acts downstream of PKC-α, mTOR, and RalA during entry.

How do RalA and mTOR recruit FlnA the plasma membranes during InlB-dependent internalization? FlnA has 24 immunoglobulin (Ig)-like repeats that interact with at least 90 different binding partners, including various receptors, cytoskeletal proteins, transcription factors, and cytoplasmic signaling proteins (18). Importantly, activated RalA binds to Ig repeat 24 in FlnA, and this interaction recruits FlnA to filopodia (37). It is plausible that the same interaction is responsible for the ability of RalA to recruit FlnA during InlB-mediated uptake. In regard to mTOR, Ig repeat 21 in FlnA is known to associate with Rictor (21, 22), an essential component of the mTOR-containing complex mTORC2 (16). mTORC2 has an important role in InlB-dependent internalization of *Listeria* (13). Future work should reveal whether mTORC2 contributes to recruitment of FlnA during InlB-mediated entry.

Our data indicate that phosphorylation of S2152 in FlnA participates in InlB-mediated uptake and exocytosis. Although phosphorylation of this site controls several biological processes including protein trafficking, cell adhesion, and cell

migration, how phosphorylation affects FlnA activity is not well understood (20, 22, 30-33). There is some evidence to suggest that phosphorylation of serine 2152 augments binding of ligands to Ig repeat 21 in FlnA (40). Serine 2152 is located in Ig repeat 20 of FlnA (18). Structural and computer modeling studies provide evidence that Ig repeat 20 controls the force-dependent interaction of ligands with Ig repeat 21 in FlnA (18, 41). FlnA is an actin filament bundling protein that is subjected to mechanical forces exerted by actomyosin-mediated contractility (42). These forces lead to the displacement of a beta strand from Ig repeat 20 that would otherwise inhibit binding of ligands to Ig repeat 21 (42, 43). Interestingly, computer simulations predict that phosphorylation of serine 2152 lowers the force needed to relieve autoinhibition of binding to repeat 21 (40). Collectively, these structural, cell biological, and modeling studies suggest that phosphorylation of serine 2152A might enhance binding of ligands to Ig repeat 21 (40-43). This idea predicts that one or more ligands of Ig repeat 21 might participate in exocytosis during InlB-mediated entry.

Finally, our results indicate an important role for the host exocyst complex in entry of InlB-coated beads and in invasion of the wild-type *Listeria* strain EGD. Interestingly, strain EGD expresses higher levels of InlB than some other commonly studied strains of *Listeria* due the presence of an activated form of the transcription factor PrfA (44). In future work, it will be of interest to examine if FlnA and the exocyst complex play important roles in entry of *Listeria* strains apart from EGD. Like the *Listeria* strain EGD, the bacteria *Salmonella enterica* serovar typhimurium and *Staphylococcus aureus* exploit the exocyst complex in order to gain entry into human cells (45-47). An interesting question for future research is whether subversion of exocytosis through the exocyst is a general strategy used for internalization by bacterial pathogens.

MATERIALS AND METHODS

Bacterial strains, mammalian cell lines and media

The *Listeria monocytogenes* strain BUG 947 was grown in brain heart infusion (BHI; Difco) broth and prepared for infection as described (34). This strain is derived from the wild-type strain EGD and contains an in-frame deletion in the *inlA* gene and is internalized into mammalian cells in a manner dependent on the *Listeria* protein InlB and its host receptor Met (3, 26, 48).

The human epithelial cell line HeLa (ATTC CCL-2) was grown in Dulbecco's modified Eagle's medium (DMEM) with 4.5 g of glucose per liter and 2 mM glutamine (catalog no. 11995-065; Life Technologies), supplemented with 5 or 10% fetal bovine serum (FBS). Cell growth, bacterial infections, incubations with latex beads, and stimulation with InlB protein were performed at 37°C under 5% CO2.

Antibodies, inhibitors, and purified proteins

Rabbit antibodies used were anti-InlB(3), anti-Met (4560; Cell Signaling Technology), anti-myc (PRB-150P; Covance), and anti-phospho-Filamin A (Serine 2152) (Cell Signaling Technology; 4761). Mouse monoclonal antibodies used were, anti-Exo70 (ED2001; Kerafast), anti-Filamin A (Millipore; CBL228), anti-glutathione-S-transferase (GST) (G1160; Sigma-Aldrich), anti-GFP (11814460001; Sigma-Aldrich), anti-myc (9E10) (626802; Biolegend), normal mouse IgG (sc-2025; Santa Cruz Biotechnology), anti-Sec3 (HPA037706; Sigma-Aldrich); anti-Sec5 (ED2002; Kerafast), anti-Sec8 (610658; Becton Dickenson) and anti-tubulin (T5168; Sigma-Aldrich). Horseradish peroxidase (HRPO)-conjugated secondary antibodies were purchased from Jackson Immunolabs. Secondary antibodies or phalloidin coupled to Alexa Fluor 488, Alexa Fluor 555, or Alexa Fluor 647 were obtained from

Life Technologies. 6XHis-tagged InlB or glutathione S-transferase proteins were expressed in *E. coli* and purified as previously described (34, 49). Okadaic acid and sodium orthovanadate were purchased from Sigma-Aldrich.

siRNAs

The sequences of short interfering RNAs (siRNAs) used were 5'-GGAAUUGAGUGGUGGUAGAtt-3' (Arp3), 5'-GGUUAAAGGUGACUGAUUAuu-3' (Exo70-1), 5'-CAGACAACAUCAAGAAUGAtt-3' (Exo70-2), 5'-GACUGGCGUGUCAUUGGACAGAUAAtt-3' (Exo70-3), 5'-CAGUCAAGUUCAACGAGGAtt-3' (FlnA #1), (2) GUGACCGCCAAUAACGACAuu (FlnA #2), 5'-CGAAGAAAGCCCGUGCCUAtt-3' (FlnA #3), 5'-CCAGAGACAUGUAUGAUAAuu-3' (Met), 5'-GGAAAUGGGUUGAUGAACUtt-3' (mTOR), 5'-GCUCCACACUAAAUCCGCAtt-3' (PKC-α), 5'-CUGCAAUUAGAGACAACUAtt-3' (RalA), 5'-GAUUCAGUGAUUUGCGAGAtt-3' (Sec3-1), 5'-CACUAAACCUUGUGAAAGAtt-3' (Sec3-2), 5'-GAUUGCAUGGGCCCUUCGAtt-3' (Sec3-3), 5'-CUCAAUGUGCUUCAGCGAUtt-3' (Sec5-1), 5'-GUUAGCAUGGCCUCAUUGAtt-3' (Sec5-2), 5'-GUAAUUGCUGCUAUCUAGAtt-3' (Sec5-3), 5'-AGAACCUGCUUUCAUGCAAuu-3' (Sec8-1), 5-CUUGAUACCUCUCACUAUUtt-3' (Sec8-2), and 5'-CCAGAAACAGUUAAGGCAAtt-3' (Sec8-3). These siRNAs were obtained from Sigma-Aldrich. The negative, non-targeting control siRNA molecule #1 (catalog no.

D-001210-01) was purchased from Dharmacon. This siRNA has two or more mismatches with all sequences in the human genome, indicating that it should not target host mRNAs.

Mammalian expression plasmids

Mammalian expression vectors used were EGFPC1 (Clontech), pcDNA-myc-FlnA.wt (Addgene # 8982; gift of John Blenis), pcDNA-myc-FlnA.S2152A (Addgene # 8983; gift of John Blenis), pEGFP-C3-Exo70 (Addgene #53761; gift of Channing Der), and VAMP3-GFP (38).

Transfection

HeLa cells grown in 24 well plates or on 22- by 22-mm coverslips were transfected with siRNAs or plasmid DNA using lipofectamine 2000 (Life Technologies) as previously described (26, 50).

Coupling of proteins to latex beads

InlB or GST proteins were coupled to carboxylate-modified latex beads 3 μm in diameter (Polysciences; catalog no. 09850) using either passive binding or covalent linkage as described (6, 26).

Stimulation of mammalian cells with soluble InlB or beads coated with InlB

HeLa cells were starved by incubation in DMEM without FBS for 9-10 h followed by addition of 300 ng/ml (4.5 nM) soluble InlB for 10 min at 37˚C in 5%. In the case of experiments with beads, particles coated with InlB or GST were added at a ratio of approximately 5 beads per HeLa cell. Cells were centrifuged at 1000 rpm for 2 min to

enhance contact between beads and cells, and then incubated for 10 min at 37˚C in 5% CO_2. After incubation with soluble InlB or beads, cells were then washed in cold PBS, and lysates were prepared for Western blotting or immunoprecipitation.

Western blotting and immunoprecipitation

For experiments involving Western blotting of total cell lysates, HeLa cells were solubilized in radioimmunoprecipitation assay (RIPA) buffer (1% Triton X-100, 0.25% sodium deoxycholate, 0.05% SDS, 50 mM Tris-HCl [pH 7.5], 2 mM EDTA, 150 mM NaCl, 1 mM phenylmethylsulfonyl fluoride, and 10 mg/liter each of aprotinin and leupeptin. For experiments assessing phosphorylation of FlnA, cells were solubilized in RIPA buffer containing 3 mM sodium orthovanadate and 1 µM okadaic acid. Protein concentrations of lysates were determined using a bicinchoninic acid (BCA) assay kit (Pierce), and equal protein amounts of each sample were migrated on 7.5% SDS/polyacrylamide gels. For analysis of phosphorylation of myc-tagged FlnA proteins, cells were solubilized in lysis buffer containing 50 mM Tris-HCl pH 7.5, 150 mM NaCl, 1% Triton X-100, 2 mM EDTA, 1 mM PMSF, 1 µM okadaic acid, 1 mM vanadate, and 10 µg per ml each of aprotinin and leupeptin. Lysates were used to prepare immunoprecipitates with anti-FlnA antibody or normal mouse IgG as a control. Immunoprecipitations were performed using protein A/G agarose beads (Santa Cruz Biotechnology) as described (34). Immunoprecipitates were migrated on 7.5% SDS/polyacrylamide gels and Western blotted with anti-phospho-Filamin A (Serine 2152) antibodies. All Western blotting experiments involved transfer of samples to PVDF membranes, incubation with primary antibodies or secondary antibodies coupled to horse radish peroxidase, and detection using enhanced chemiluminescence (ECL) or ECL Plus reagents (GE Healthcare), as

described previously (3). Chemiluminescence was detected using an Odyssey imaging system (Li-Cor Biosciences). Bands in Western blot images were quantified using ImageJ software as described (51).

Bacterial invasion assays

Invasion of *Listeria* was measured using gentamicin protection assays, as previously described (3, 29). HeLa cells were infected with *Listeria* approximately 48 h after transfection with siRNAs. Cells were infected for 1 h in the absence of gentamicin using a multiplicity of infection of 30:1, and then incubated in DMEM with 20 µg/ml gentamicin for an additional 2 h. Bacterial invasion efficiencies were first expressed as the percentage of the inoculum that survived gentamicin treatment. To obtain relative invasion values, absolute percent entry values in a given experiment were normalized to the value in cells subjected to mock transfection in the absence of siRNA.

Quantification of internalization of beads

Beads coated with InlB or GST were added to HeLa cells growing on 22- by 22-mm coverslips. A ratio of approximately 5 particles to human cells was used. Cells were centrifuged at 1000 rpm for 2 min at room temperature and then incubated for 30 min at 37˚C in 5% CO_2 to allow internalization of beads. Cells were then washed in PBS and fixed in PBS containing 3% paraformaldehyde (PFA). Samples were labeled with anti-InlB or anti-GST antibodies, using a previously described approach that distinguishes extracellular or intracellular particles (26). In the case of experiments involving myc-tagged FlnA proteins (Fig. 3A,B,C), samples were also labeled with mouse anti-myc antibodies to allow identification of transfected cells. Secondary

antibodies used for labeling were coupled to Alexa Fluor 488, Alexa Fluor 555, and Alexa Fluor 647. Labeled samples were mounted in Molwiol with 1,4-diazabicyclo[2.2.2]octane (DABCO) as an anti-fade agent. Samples were analyzed for intracellular and extracellular beads using an Olympus BX51 epifluorescence microscope equipped with a 20x 0.75 NA dry objective lens and an Olympus DP80 CCD camera, using Olympus cellSens software (version 1.13). The data shown in Figures 1C, 3B, and S1 are from three experiments. In each experiment, at least 100 intracellular beads were scored for the control conditions involving mock transfection in the absence of siRNA. A similar number of total (intracellular plus extracellular) beads were analyzed for all other conditions. Data were initially expressed as the percentage of total cell-associated beads that were internalized. These data were then converted to relative internalization values by normalizing to percent internalization data from controls lacking siRNA.

Confocal microscopy analysis

For studies involving exocytosis in Figures 5 and 9, HeLa cells grown on 22- x 22-mm coverslips were transfected with siRNAs and then transfected again 24 h later with a plasmid expressing VAMP3 fused to GFP (VAMP3-GFP). Approximately 24 h after addition of plasmid DNA, cells were washed, placed in serum-free DMEM, and incubated for 5 min in serum-free DMEM with InlB- or GST-coated beads, as described above. HeLa cells were washed in PBS and incubated with mouse anti-GFP antibodies for 1 h at 4˚C. Cells were then fixed in PBS with 3% PFA, and incubated with anti-mouse antibodies coupled to Alexa Fluor 647 for 1 h. This method resulted in labeling of exofacial VAMP3-GFP (6, 38). Extracellular beads were labeled by incubation with anti-InlB or anti-GST antibodies, followed by secondary antibodies

conjugated to Alexa Fluor 555. Experiments to determine effect of myc-tagged FlnA proteins on exocytosis (Fig. 6) were performed similarly to the exocytosis studies described above, except that HeLa cells were co-transfected with plasmids expressing VAMP3-GFP and either myc-FlnA.wt or myc-FlnA-S2152A. After exofacial labeling of VAMP3-GFP with mouse anti-GFP antibodies, cells were permeabilized in PBS containing 0.4% Triton X-100, and myc-tagged proteins were labeled with rabbit anti-myc antibodies and anti-rabbit-Alexa Fluor 555. Experiments assessing recruitment of GFP-Exo70 (Fig. 8) were performed similarly to the exocytosis experiments, except that the exofacial labelling step with anti-GFP antibodies was omitted. For labeling of endogenous Exo70, Sec5, or Sec8 (Fig. S2B), cells were fixed by incubation in methanol for 5 min at -20˚C. Samples were then incubated overnight at 4˚C with primary antibodies in PBS with 1.0% BSA and 0.1% Tween 20.

All samples analyzed by confocal microscopy were mounted in Molwiol supplemented with DABCO. Imaging was performed with an inverted Olympus FV1200 laser scanning confocal microscope, using a 60x 1.35 NA oil immersion objective, laser lines of 488 nm, 543 nm, and 633 nm, and photomultiplier tubes for detection. Images from serial sections spaced 1.0 µm apart were used to ensure that all cell-associated beads were detected. Image J (version 1.51e) software was employed to determine fold enrichment (FE) values for each cell-associated bead. FE is defined as the mean pixel intensity in a ring-like structure around the bead, normalized to the mean pixel intensity throughout the human cell (6, 13, 28, 29). The thresholding function of Image J was used to measure mean pixel intensities in ring-like structures of FlnA, exofacial VAMP3-GFP, or GFP-Exo70 around beads. This function was also used to measure mean pixel intensity throughout the cell. In each experiment, approximately 50-100 extracellular, cell-associated beads were analyzed

for each condition. The data shown in Figures 4B, 5B, 6B, 8B, and 9B are pooled FE values from three or four independent experiments.

Statistical analysis

Statistical analysis was performed using Prism (version 6.0c; GraphPad Software). In comparisons of data from three or more conditions, analysis of variance (ANOVA) was used. The Tukey-Kramer test was used as a posttest. For comparisons of two data sets, Student's t-test was used. A P-value of 0.05 or lower was considered significant.

ACKNOWLEDGEMENTS

We thank Segolene de Champs for initial imaging studies with GFP-tagged exocyst proteins. This work was supported by grants from the Marsden Fund of the Royal Society of New Zealand (13-UOO-085), the Health Research Council of New Zealand (17/082), the University of Otago Research Committee, and the Dean's Bequest Fund (Otago School of Biomedical Sciences, University of Otago), awarded to K. Ireton.

514 **FIGURE LEGENDS**

515 **Figure 1.** ***Host FlnA promotes InlB-mediated entry.*** HeLa cells were either mock
516 transfected in the absence of siRNA, transfected with a control non-targeting siRNA,
517 or transfected with three different siRNAs against FlnA. About 48 h after transfection,
518 cell lysates were prepared for analysis of target gene expression by Western blotting,
519 or cells were incubated with *Listeria* or InlB-coated beads for assessment of invasion
520 or entry, respectively. A. Effect of siRNAs against FlnA on target protein expression.
521 A representative blot showing depletion of FlnA is displayed. After reaction with anti-
522 FlnA antibodies, the membrane was stripped and probed with anti-tubulin antibodies
523 to confirm equivalent loading. The adjacent bar graph displays mean +/- SEM values
524 of quantified Western blotting data from three independent experiments. B. Effect of
525 siRNAs targeting FlnA on invasion of *Listeria* expressing InlB. Results are mean +/-
526 SEM relative entry values from three to six independent gentamicin protection
527 experiments, depending on the condition. C. Effect of an siRNA targeting FlnA on
528 entry of InlB-coated beads. (i). Internalization of beads coated with InlB or GST into
529 HeLa cells. Data are the mean percentage of total cell-associated beads internalized
530 +/- SEM from three independent experiments. 'ND' indicates that no internalized
531 beads were detected. (ii). Decreased entry of InlB-coated beads into HeLa cells
532 transfected with FlnA siRNA. The siRNA against FlnA used was #2. Results are
533 mean relative entry values +/- SEM from three independent experiments. *, $P < 0.05$
534 compared to the control siRNA condition, as determined by ANOVA and the Tukey-
535 Kramer posttest.

536

537 **Figure 2.** ***InlB stimulates PKC-α -dependent phosphorylation of FlnA.*** A.
538 Specificity of anti-phospho-FlnA antibodies. (i). Effect of FlnA RNAi on reactivity

with antibodies. HeLa cells were either transfected with a control siRNA or with an siRNA targeting FlnA. Cell lysates were prepared and used for Western blotting with antibodies that recognize phosphorylated serine 2152 in FlnA. The left panel shows a representative Western blot and the right panel displays quantified Western blotting data as mean +/- SEM values from three independent experiments. (ii). Effect of mutation of serine 2152 on antibody reactivity. HeLa cells were transfected with plasmids expressing myc-tagged wild-type (wt) FlnA or FlnA containing a serine-to-alanine substitution in residue 2152 (S2152A). After transfection, lysates were prepared and used for immunoprecipitation with anti-myc antibodies or mock precipitation with control IgG. Precipitates were Western blotted using anti-phospho-FlnA (serine 2152) antibodies. Shown is a representative Western blot from one of two experiments performed. (B). Effect of depletion of PKC-α on phosphorylation of FlnA. After transfection of HeLa cells with control siRNA or an siRNA against PKC-α, lysates were prepared and used for Western blotting with antibodies against phosphorylated serine 2152 in FlnA, total FlnA, PKC-α, or tubulin. (i). Representative Western blots are shown. (ii). Quantified Western blotting data expressed as mean +/- SEM values from six independent experiments are presented. (C). Effect of depletion of Met on phosphorylation of FlnA. (i). Representative Western blotting results are shown. (ii). Quantified Western blotting data expressed as mean +/- SEM values from seven independent experiments are displayed. (D). Phosphorylation of FlnA during InlB-mediated entry. HeLa cells were incubated with latex beads coupled to InlB or GST for 10 min, followed by solubilization in lysis buffer. Lysates were Western blotted with anti-phospho-FlnA (serine 2152) antibodies. (i). A representative Western blot is shown. (ii). Quantified Western

563 blotting data expressed as mean +/- SEM values from three independent experiments
564 are presented. *, P < 0.05, as determined by ANOVA and the Tukey-Kramer posttest.
565
566 **Figure 3.** ***Phosphorylation of FlnA on serine 2152 contributes to InlB-mediated***
567 ***entry***. HeLa cells were transfected with plasmids expressing myc-tagged wild-type
568 (WT) FlnA or FlnA containing a serine-to-alanine substitution in residue 2152
569 (S2152A). About 24 h after transfection, lysates were prepared for evaluation of
570 tagged FlnA protein expression by Western blotting or fixed samples were made for
571 fluorescence microscopy analysis of entry of InlB-coated beads. A. Expression of
572 myc-tagged FlnA proteins assessed by Western blotting. The panel on the left shows a
573 representative Western blot, whereas the graph on the right displays quantified
574 Western blotting data as mean +/SEM values from three independent experiments. B.
575 Entry of InlB-coated beads. (i). The percentage of cell-associated beads that were
576 internalized into HeLa cells expressing myc-tagged FlnA.WT or FlnA.S2152A
577 proteins is shown. (ii). Expression of myc-tagged FlnA proteins in the same samples
578 used for analysis of internalization of InlB-coated beads. Pixel intensities in HeLa
579 cells associated with InlB-coated beads were quantified using Image J software. The
580 data in (i) and (ii) are mean +/- SEM values from four independent experiments. *, P,
581 < 0.05, as determined by Student's t-test.
582
583 **Figure 4.** ***FlnA is recruited during entry in a manner that depends on mTOR, RalA,***
584 ***and Met.*** HeLa cells were mock transfected in the absence of siRNA, transfected with
585 a control siRNA, or transfected with siRNAs targeting mTOR, PKC-α, RalA, or Met.
586 Cells were then incubated for 10 min with beads coupled to InlB or to GST, followed
587 by fixation and labeling for confocal microscopy. A. Confocal microscopy images of

588 localization of endogenous FlnA. Panels on the left show FlnA localization in HeLa
589 cells, with locations of beads indicated with arrows. Regions near beads are expanded
590 in the middle and right panels. Middle panels show FlnA labeling, whereas right
591 panels are differential interference contrast (DIC) images displaying beads. Scale bars
592 indicate 5 micrometers. B. Quantification of recruitment of FlnA. Data are pooled
593 fold enrichment (FE) values from four independent experiments. Each dot represents
594 a single FE value. Horizontal bars are means and error bars are SD. *, P, < 0.05
595 compared to the no siRNA and control siRNA conditions.
596
597 **Figure 5.** ***mTOR, PKC-α, and FlnA control exocytosis during InlB-mediated entry.***
598 HeLa cells were mock transfected in the absence of siRNA, transfected with a control
599 siRNA, or transfected with siRNAs targeting mTOR, PKC-α, FlnA, Met, or Arp3.
600 Cells were then transfected with a plasmid expressing the exocytic probe VAMP3-
601 GFP and incubated for 5 min with beads coupled to InlB or to GST. Samples were
602 fixed and labeled for confocal microscopy. A. Representative confocal microscopy
603 images. Total VAMP3-GFP is green, exofacial VAMP3-GFP is red, and beads are
604 blue. Panels on the left are merged images of single HeLa cells, with locations of
605 beads indicated with arrows. Regions near beads are expanded in panels to the right.
606 Scale bars indicate 5 micrometers. B. Quantification of exocytosis. Data are pooled
607 FE values of exofacial VAMP3-GFP from three to four independent experiments,
608 depending on the condition. Dots represent individual FE values. Horizontal bars are
609 means and error bars are SD. *, P < 0.05 compared to the control siRNA condition, as
610 determined by ANOVA and the Tukey-Kramer posttest.
611
612 **Figure 6.** ***Phosphorylation of serine 2152 in FlnA contribute to exocytosis.***

HeLa cells were co-transfected with plasmids expressing VAMP3-GFP and either myc-tagged wild-type (wt) FlnA or FlnA.S2152A. Cells were then incubated with InlB-coated beads for 5 min, followed by labeling for exofacial VAMP3-GFP and myc-tagged proteins. Confocal microscopy was performed to acquire images for quantification of exocytosis. A. Representative microscopy images. Myc-tagged FlnA proteins are colored blue, VAMP3-GFP is green, exofacial VAMP3-GFP is red, and beads are detected using differential interference contrast (DIC) microscopy. Panels on the left are merged images of single HeLa cells, with locations of beads indicated with arrows. Regions near beads are expanded in panels to the right. Scale bars indicate 5 micrometers. B. (i). Quantification of exocytosis. Data are pooled FE values of exofacial VAMP3-GFP from three independent experiments. Dots represent individual FE values. Horizontal bars are means and error bars are SD. (ii). Expression of myc-tagged FlnA proteins in the same samples used for analysis of exocytosis. Pixel intensities in HeLa cells associated with InlB-coated beads were quantified using Image J software. The data are mean pixel intensities +/- SEM from three independent experiments. *, $P < 0.05$, as determined by Student's t-test.

Figure 7. ***The exocyst complex promotes InlB-dependent invasion of Listeria.*** HeLa cells were mock transfected in the absence of siRNA, transfected with a control siRNA, or transfected with siRNAs against the exocyst components Sec3, Sec5, Sec8, or Exo70. About 48 h after transfection, cells were solubilized for assessment of target protein expression or infected with wild-type *Listeria* for analysis of invasion. A. Effect of siRNAs on Sec3 expression and invasion of *Listeria*. (i). Sec3 expression. The left panel shows a representative Western blot indicating depletion of Sec3 by siRNAs. The right panel is quantified Western blotting data showing mean relative

638 Sec3 expression +/- SEM from three independent experiments. (ii). Invasion of
639 *Listeria*. Data are mean relative entry values +/- SEM from three to eight independent
640 experiments, depending on the siRNA. B. siRNA-mediated inhibition in Sec5
641 expression and invasion of *Listeria*. (i). Sec5 expression. In the left panel, a
642 representative Western blot is shown. The right panel displays quantified Western
643 blotting data from three independent experiments. (ii). Invasion of *Listeria*. Data are
644 means +/- SEM from three to six independent experiments. C. Reduction in
645 expression of Sec8 and invasion of *Listeria* by siRNAs. (i). Sec8 expression. (i). In
646 the left panel, a representative Western blot is presented. The right panel shows
647 quantified Western blotting data from three independent experiments. (ii). Invasion of
648 *Listeria*. Data are means +/- SEM of three to six independent experiments. D. siRNA-
649 mediated inhibition in expression of Exo70 and invasion of *Listeria*. (i). Exo70
650 expression. The left panel shows a representative Western blot and the right panel
651 displays quantitative Western blotting data from three independent experiments. (ii).
652 Invasion of *Listeria*. Data are means +/- SEM from three independent experiments. *,
653 $P < 0.05$, as determined by ANOVA and the Tukey-Kramer posttest.
654
655 **Figure 8.** ***mTOR, PKC-α, RalA, and FlnA mediate recruitment of Exo70 during***
656 ***InlB-mediated entry***. HeLa cells were subjected to control conditions or transfected
657 with siRNAs against mTOR, PKC-α, RalA, FlnA, Met, or Arp3. Cells were then
658 transfected with a plasmid expressing Exo70 fused to GFP (GFP-Exo70). After
659 transfection, cells were incubated for 5 min with beads coupled to InlB or to GST,
660 followed by fixation and labeling for confocal microscopy. A. Representative
661 confocal microscopy images. GFP-Exo70 is green and beads are red. Panels on the
662 left are merged images of single HeLa cells. Arrows indicate beads. Regions near

beads are expanded in the panels to the right. Scale bars indicate 5 micrometers. B. Quantification of recruitment of GFP-Exo70. Data are pooled FE values of GFP-Exo70 from three independent experiments. Dots represent individual FE values. Horizontal bars are means and error bars are SD. *, $P < 0.05$ compared to the control siRNA condition, as assessed by ANOVA and the Tukey-Kramer posttest.

Figure 9. ***The exocyst complex promotes exocytosis during InlB-mediated entry*****.** HeLa cells were subjected to control conditions or transfected with siRNAs against Sec3, Sec5, Sec8, or Exo70. Cells were then transfected with a plasmid expressing VAMP3-GFP. After transfection, cells were incubated for 5 min with beads coupled to InlB, followed by fixation and labeling for confocal microscopy. Scale bars indicate 5 micrometers. A. Representative confocal microscopy images. Total VAMP3-GFP is green, exofacial VAMP3-GFP is red, and beads are blue. Panels on the left are merged images of single HeLa cells, with beads being indicated by arrows. Regions near beads are expanded in panels to the right. B. Quantification of exocytosis. Data are pooled FE values of exofacial VAMP3-GFP from three independent experiments. Dots represent individual FE values. Horizontal bars are means and error bars are SD. *, P, < 0.05 compared to the no siRNA or control siRNA conditions, as determined by ANOVA and the Tukey-Kramer posttest.

685
686

REFERENCES

687 1. Posfay-Barbe KM, Wald ER. 2009. Listeriosis. Semin Fetal Neonatal Med
688 14:228-233. https://doi.org/10.1016/j.siny.2009.01.006.
689 2. Disson O, Lecuit M. 2013. *In vitro* and *in vivo* models to study human
690 listeriosis: mind the gap. Microbes Infect 15:971-980.
691 https://doi.org/10.1016/j.micinf.2013.09.012.
692 3. Shen Y, Naujokas M, Park M, Ireton K. 2000. InlB-dependent internalization
693 of Listeria is mediated by the Met receptor tyrosine kinase. Cell 103:501-510.
694 https://doi.org/10.1016/S0092-8674(00)00141-0.
695 4. Pizarro-Cerda J, Kühbacher A, Cossart P. 2012. Entry of Listeria
696 monocytogenes in mammalian epithelial cells: an updated view. Cold Spring
697 Harb Perspect Med 2:a010009. https://doi.org/ 10.1101/cshperspect.a010009.
698 5. Kuhbacher A, Emmenlauer M, Ramo P, Kafai N, Dehio C, Cossart P, Pizarro-
699 Cerda J. 2015. Genome-wide siRNA screeen identifies complementary
700 signaling pathways involved in Listeria infection and reveals different actin
701 nucleation mechanisms during Listeria cell invasion and actin comet tail
702 formation. mBio 6:e00598-00515. https://doi.org/10.1128/mBio.00598-15.
703 6. Van Ngo H, Bhalla M, Chen DY, Ireton K. 2017. A role for host exocytosis in
704 InlB-mediated entry of Listeria monocytogenes. Cell Microbiol 19:e12768.
705 https://doi.org/10.1111/cmi.12768.
706 7. Ireton K, Rigano LA, Dowd GC. 2014. Role of host GTPases in infection by
707 Listeria monocytogenes. Cell Microbiol 16:1311-1320. https://doi.org/
708 10.1111/cmi.12324.
709 8. Hong WJ, Lev S. 2014. Tethering the assembly of SNARE complexes. Trends
710 Cell Biol 24:35-43. https://doi.org/10.1016/j.tcb.2013.09.006.

9. Daumke O, Roux A, Haucke V. 2014. BAR domain scaffolds in Dynamin-mediated membrane fission. Cell 156:882-892. https://doi.org/10.1016/j.cell.2014.02.017.
10. Veiga E, Cossart P. 2005. Listeria hijacks the clathrin-dependent endocytic machinery to invade mammalian cells. Nat Cell Biol 7:894-900. https://doi.org/10.1038/ncb1292.
11. Bierne H, Gouin E, Roux P, Caroni P, Yin HL, Cossart P. 2001. A role for cofilin and LIM kinase in Listeria-induced phagocytosis. Journal of Cell Biology 155:101-112. https://doi.org/10.1083/jcb.200104037.
12. Bierne H, Miki H, Innocenti M, Scita G, Gertler FB, Takenawa T, Cossart P. 2005. WASP-related proteins, Abi and Ena/VASP are required for Listeria invasion induced by the Met receptor. J Cell Sci 118:1537-1547. . https://doi.org/10.1242/jcs.02285.
13. Bhalla M, Law D, Dowd GC, Ireton K. 2017. Host serine-threonine kinases mTOR and Protein Kinase C-α promote InlB-mediated entry of Listeria monocytogenes. Infect Immun 85:pii: e00087-00017. https://doi.org/10.1128/IAI.00087-17.
14. Bracho-Valdes I, Moreno-Alvarez P, Valencia-Martinez I, Robles-Molina E, Chavez-Vargas L, Vazquez-Prado J. 2011. mTORC1- and mTORC2-interacting proteins keep their multifunctional partners focused. IUBMB Life 63:896-914. https://doi.org/10.1002/iub.558.
15. Morrison MM, Young CD, Wang S, Sobolik T, Sanchez VM, Hicks DJ, Cook RS, Brantley-Sieders DM. 2015. mTOR directs breast morphogenesis through the PKC-alpha-Rac1 Signaling Axis. PLoS Genet 11:e1005291. https://doi.org/10.1371/journal.pgen.1005291.

16. Gaubitz C, Prouteau M, Kusmider B, Loewith R. 2016. TORC2 Structure and Function. Trends Biochem Sci 41:532-545. https://doi.org/10.1016/j.tibs.2016.04.001.

17. Wu B, Guo W. 2015. The exocyst at a glance. J Cell Sci 128 2957-2964. https://doi.org/doi: 10.1242/jcs.156398.

18. Razinia Z, Makela T, Ylanne J, Calderwood DA. 2012. Filamins in mechanosensing and signaling. Annu Rev Biophys 41:227-246. https://doi.org/10.1146/annurev-biophys-050511-102252.

19. Tigges U, Koch B, Wissing J, Jockush BM, Ziegler WH. 2003. The F-actin cross-linking and focal adhesion protein filamin A is a ligand and in vivo substrate for protein kinase C alpha. J Biol Chem 278:23561-23569. https://doi.org/10.1074/jbc.M302302200.

20. Muriel O, Echarri A, Hellriegel C, Pavon DM, Beccari L, Del Pozo MA. 2011. Phosphorylated filamin A regulates actin-linked caveolae dynamics. J Cell Sci 124:2763-2776. https://doi.org/10.1242/jcs.080804.

21. Chantaravisoot N, Wongkongkathep P, Loo JA, Mischel PS, Tamanoi F. 2015. Significance of filamin A in mTORC2 function in glioblastoma. Mol Cancer 14:127. https://doi.org/doi: 10.1186/s12943-015-0396-z.

22. Sato T, Ishii J, Ota Y, Sasaki E, Shibagaki Y, Hattori S. 2016. Mammalian target of rapamycin (mTOR) complex 2 regulates filamin A-dependent focal adhesion dynamics and cell migration. Genes Cells 21:579-593. https://doi.org/10.1111/gtc.12366.

23. Mohr SE, Smith JA, Shamu CE, Neumuller RA, Perrimon N. 2014. RNAi screening comes of age: improved techniques and complementary approaches. Nat Rev Mol Cell Biol 15:591-600. https://doi.org/ 10.1038/nrm3860.

24. Braun L, Ohayon H, Cossart P. 1998. The InIB protein of Listeria monocytogenes is sufficient to promote entry into mammalian cells. Molecular Microbiology 27:1077-1087. https://doi.org/10.1046/j.1365-2958.1998.00750.x

25. Seveau S, Bierne H, Giroux S, Prevost MC, Cossart P. 2004. Role of lipid rafts in E-cadherin- and HGF-R/Met-mediated entry of *Listeria monocytogenes* into host cells. J Cell Biol 166:743-753. https://doi.org/10.1083/jcb.200406078.

26. Dokainish H, Gavicherla B, Shen Y, Ireton K. 2007. The carboxyl-terminal SH3 domain of the mammalian adaptor CrkII promotes internalization of Listeria monocytogenes through activation of host phosphoinositide 3-kinase. Cell Microbiol 10:2497-2516. https://doi.org/10.1111/j.1462-5822.2007.00976.x.

27. Veiga E, Guttman JA, Bonazzi M, Boucrot E, Toledo-Arana A, Lin Ae, Enninga J, Pizarro-Cerda J, Finlay BB, Kirchhausen T, Cossart P. 2007. Invasive and adherent bacterial pathogens co-opt hos clathrin for infection. Cell Host Microbe 2:340-351. https://doi.org/10.1016/j.chom.2007.10.001.

28. Gavicherla B, Ritchey L, Gianfelice A, Kolokoltsov AA, Davey RA, Ireton K. 2010. Critical role for the host GTPase-activating protein ARAP2 in InlB-mediated entry of Listeria monocytogenes. Infect Immun 78:4532-4541. https://doi.org/doi: 10.1128/IAI.00802-10.

29. Dowd GC, Bhalla M, Kean B, Thomas R, Ireton K. 2016. Role of host type IA Phosphoinositide 3-kinase pathway components in invasin-mediated internalization of Yersinia enterocolitica. Infect Immun 84:1826-1841. https://doi.org/10.1128/IAI.00142-16.

30. Vadlamudi RK, Li F, Adam L, Nguyen D, Ohta Y, Stossel TP, Kumar R. 2002. Filamin is essential in actin cytoskeletal assembly mediated by p21-activated kinase 1. Nat Cell Biol 4:681-690. https://doi.org/10.1038/ncb838.

31. Maceyka M, Alvarez SE, Milstien S, Spiegel S. 2008. Filamin A links sphingosine kinase 1 and sphingosine-1-phosphate receptor 1 at lamellipodia to orchestrate cell migration. Mol Cell Biol 28:5687-5697. https://doi.org/doi:10.1128/MCB.00465-08.

32. Li L, Lu Y, Stemmer PM, Chen F. 2015. Filamin A phosphorylation by Akt promotes cell migration in response to arsenic. Oncotarget 6:12009-12019. https://doi.org/10.18632/oncotarget.3617.

33. Pons M, Izquierdo I, Andreu-Carbo M, Garrido G, Planaguma J, Muriel O, Del Pozo MA, Geli MI, Aragay AM. 2017. Phosphorylation of filamin A regulates chemokine receptor CCR2 recycling. J Cell Sci 130:490-501. https://doi.org/ 10.1242/jcs.193821.

34. Ireton K, Payrastre B, Cossart P. 1999. The Listeria monocytogenes protein InlB is an agonist of mammalian phosphoinositide-3-kinase. J Biol Chem 274:17025-17032. https://doi.org/10.1074/jbc.274.24.17025.

35. Sun H, Shen Y, Dokainish H, Holgado-Madruga M, Wong A, Ireton K. 2005. Host adaptor proteins Gab1 and CrkII promote InlB-dependent entry of Listeria monocytogenes. Cell Microbiol 7:443-457. https://doi.org/10.1111/j.1462-5822.2004.00475.x.

36. Woo MS, Ohta Y, Rabinovitz I, Stossel TP, Blenis J. 2004. Ribosomal S6 kinase (RSK) regulates phosphorylation of filamin A on an important regulatory site. Mol Cell Biol 24:3025-3035. https://doi.org/10.1128/MCB.24.7.3025-3035.2004.

811 37. Ohta Y, Suzuki N, Nakamura S, Hartwig JH, Stossel TP. 1999. The small
812 GTPase RalA targets filamin to induce filopodia. Proc Natl Acad Sci USA
813 96:2122-2128. https://doi.org/10.1073/pnas.96.5.2122.
814 38. Bajno L, Peng XR, Schrieber AD, Moore HP, Trimble WS, Grinstein S. 2000.
815 Focal exocytosis of VAMP3-containing vesicles at sites of phagosome
816 formation. J Cell Biol 149:697-705. https://doi.org/10.1083/jcb.149.3.697.
817 39. Gentry LR, Martin TD, Reiner DJ, Der CJ. 2014. Ral small GTPase signaling
818 and oncogenesis: More than just 15 minutes of fame. Biochim Biophys Acta
819 1843:2976-2988. https://doi.org/10.1016/j.bbamcr.2014.09.004.
820 40. Chen HS, Kolahi KS, Mofrad MRK. 2009. Phosphorylation facilitates the
821 integrin binding of filamin under force. Biophys J 97:3095-3104.
822 https://doi.org/10.1016/j.bpj.2009.08.059.
823 41. Lad Y, Kiema T, jiang P, Pentikainen OT, Coles CH, Campbell ID,
824 Calderwood DA, Ylanne J. 2007. Structure of three tandem filamin domains
825 reveals auto-inhibition of ligand binding. EMBO J 26:3993-4004.
826 https://doi.org/10.1038/sj.emboj.7601827.
827 42. Nakamura F, Song M, Hartwig JH, Stossel TP. 2014. Documentation and
828 localization of force-mediated filamin A domain perturbations in moving
829 cells. Nat Commun 5:4656. https://doi.org/10.1038/ncomms5656.
830 43. Pentikainen U, Ylanne J. 2009. The regulation mechanism for the auto-
831 inhibition of binding of human Filamin A to integrin. J Mol Biol 393:644-657.
832 https://doi.org/10.1016/j.jmb.2009.08.035.
833 44. Becavin C, Bouchier C, Lechat P, Archambaud C, Creno S, Gouin E, Wu Z,
834 Kuhbacher A, Brisse S, Pucciarelli G, Garcia-del Portillo F, Hain T, Portnoy
835 DA, Chakraborty T, Lecuit M, Pizarro-Cerda J, Mozner, I, Bierne, H, Cossart

P. 2014. Comparison of widely used Listeria monocytogenes strains EGD, EGDe, 10403S, and EGD-e highlights genomic differences underlying variations in pathogenicity. mBio 5:e00969-14. https://doi.10.1128/mBio.00969-14

45. Nichols CD, Casanova JE. 2010. Salmonella-directed recruitment of new membrane to invasion foci via the host exocyst complex. Curr Biol 20:1316-1320. https://doi: 10.1016/j.cub.2010.05.065.

46. Rauch L, Hennings K, Trasak C, Roder A, Schroder B, Koch-Nolte F, Rivera-Molina F, Toomre D, Aepfelbacher M. 2016. Staphylococcus aureus recruits Cdc42GAP through recycling endosomes and the exocyst to invade human endothelial cells. J Cell Sci 129:2937-2949. https://doi.org/10.1242/jcs.186213.

47. Ireton K, Van Ngo H, Bhalla M. 2018. Interaction of microbial pathogens with host exocytic pathways. Cell Microbiol 20:e12861. https://doi.org/ doi: 10.1111/cmi.12861.

48. Dramsi S, Biswas I, Maguin E, Braun L, Mastroeni P, Cossart P. 1995. Entry of *Listeria monocytogenes* into hepatocytes requires expression of inIB, a surface protein of the internalin multigene family. Mol Microbiol 16:251-261. https://doi.org/ https://10.1111/j.1365-2958.1995.tb02297.x.

49. Basar T, Shen Y, Ireton K. 2005. Redundant roles for Met docking site tyrosines and the Gab1 pleckstrin homology domain in InlB-mediated entry of Listeria monocytogenes. Infect Immun 73:2061-2074. https://doi.org/10.1128/IAI.73.4.2061-2074.2005.

50. Jiwani S, Wang Y, Dowd GC, Gianfelice A, Pichestapong P, Gavicherla B, Vanbennekom N, Ireton K. 2012. Identification of components of the type IA

phosphoinositide 3-kinase pathway that promote internalization of Listeria monocytogenes. Infect Immun 80:1252-1266. https://doi.org/10.1128/IAI.06082-11.

51. Gianfelice A, Le PH, Rigano LA, Saila S, Dowd GC, McDivitt T, Bhattacharya N, Hong W, Stagg SM, Ireton K. 2015. Host endoplasmic reticulum COPII proteins control cell-to-cell spread of the bacterial pathogen Listeria monocytogenes. Cell Microbiol 17:876-892. https://doi.org/10.1111/cmi.12409.

Figure 1

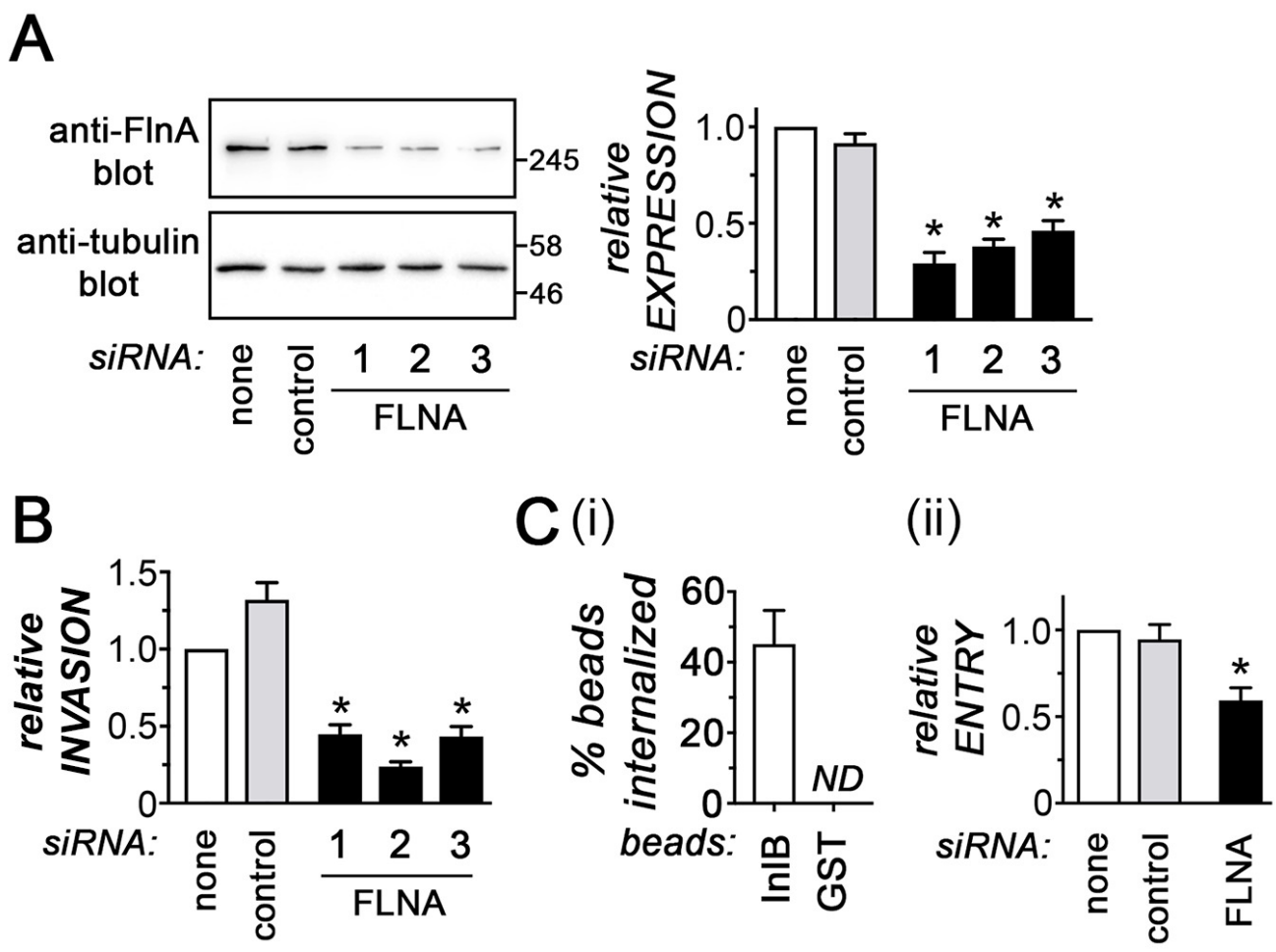

Figure 2

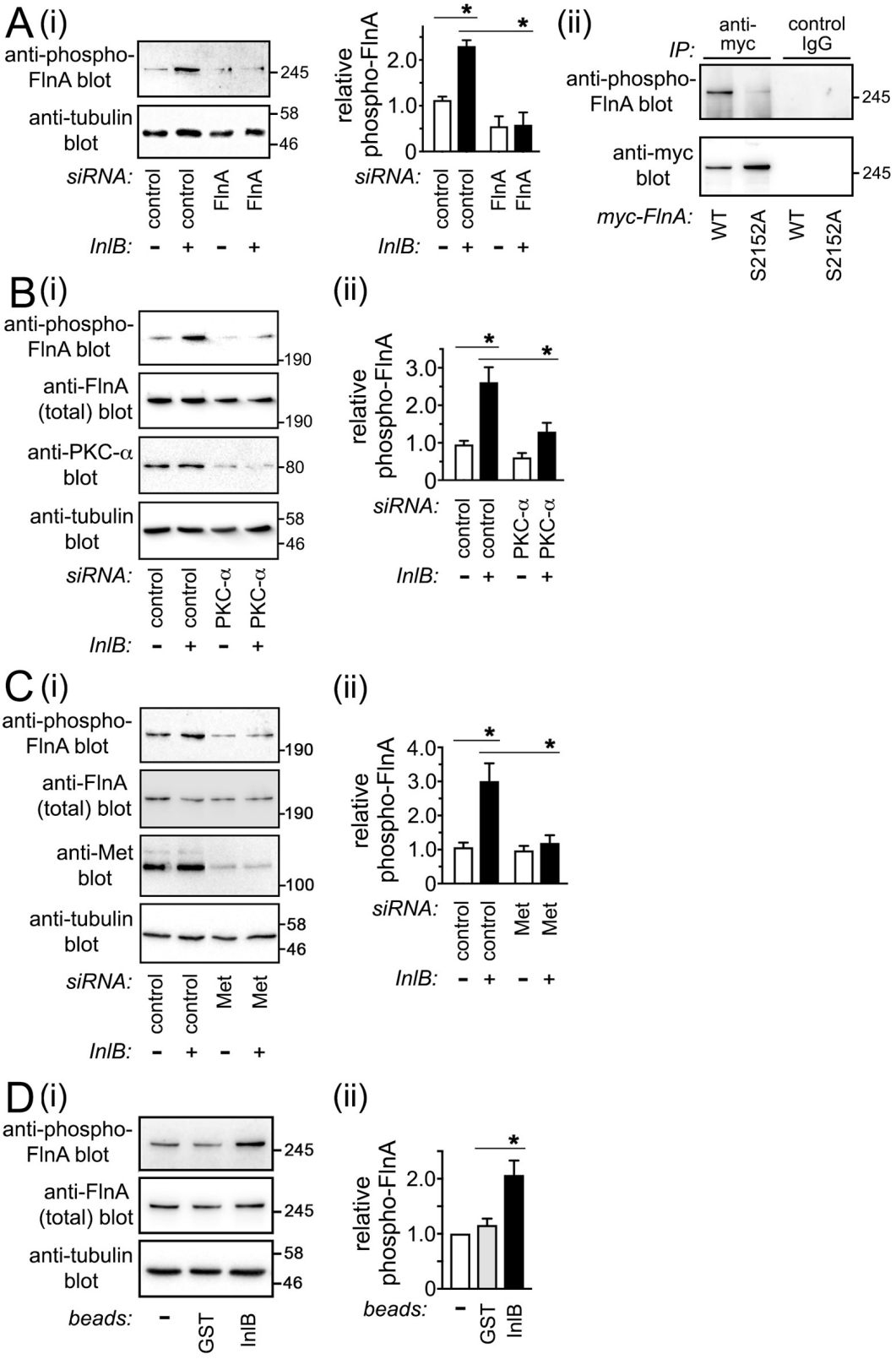

Figure 3

Figure 4

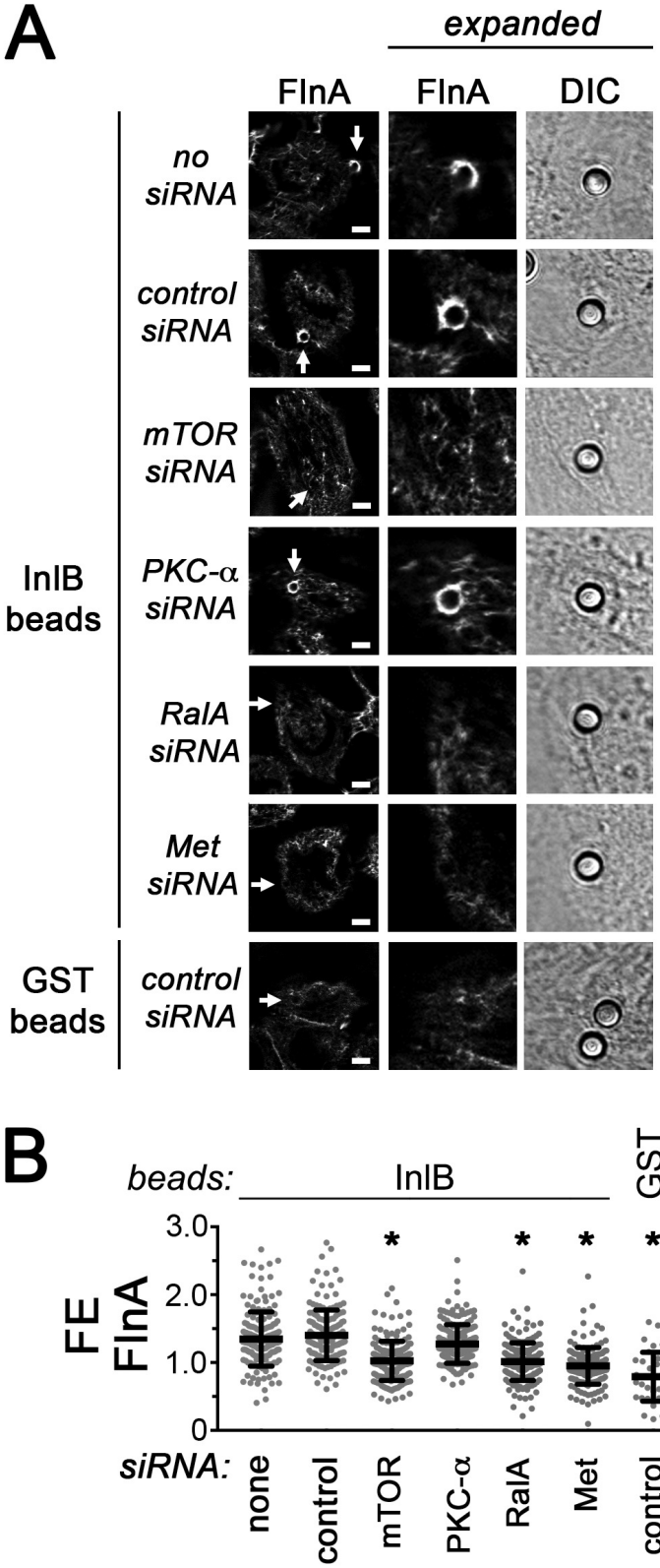

Figure 5

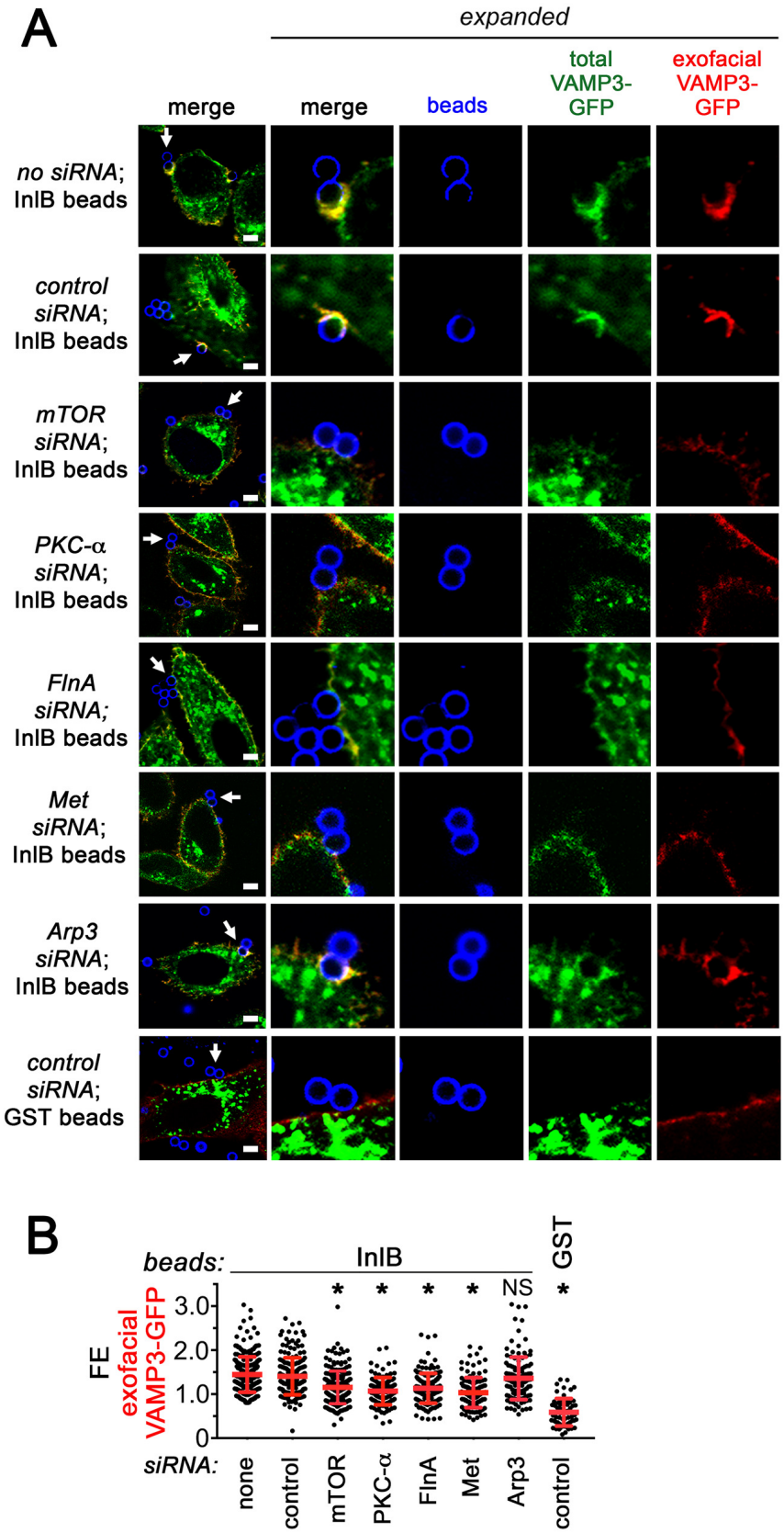

Figure 6

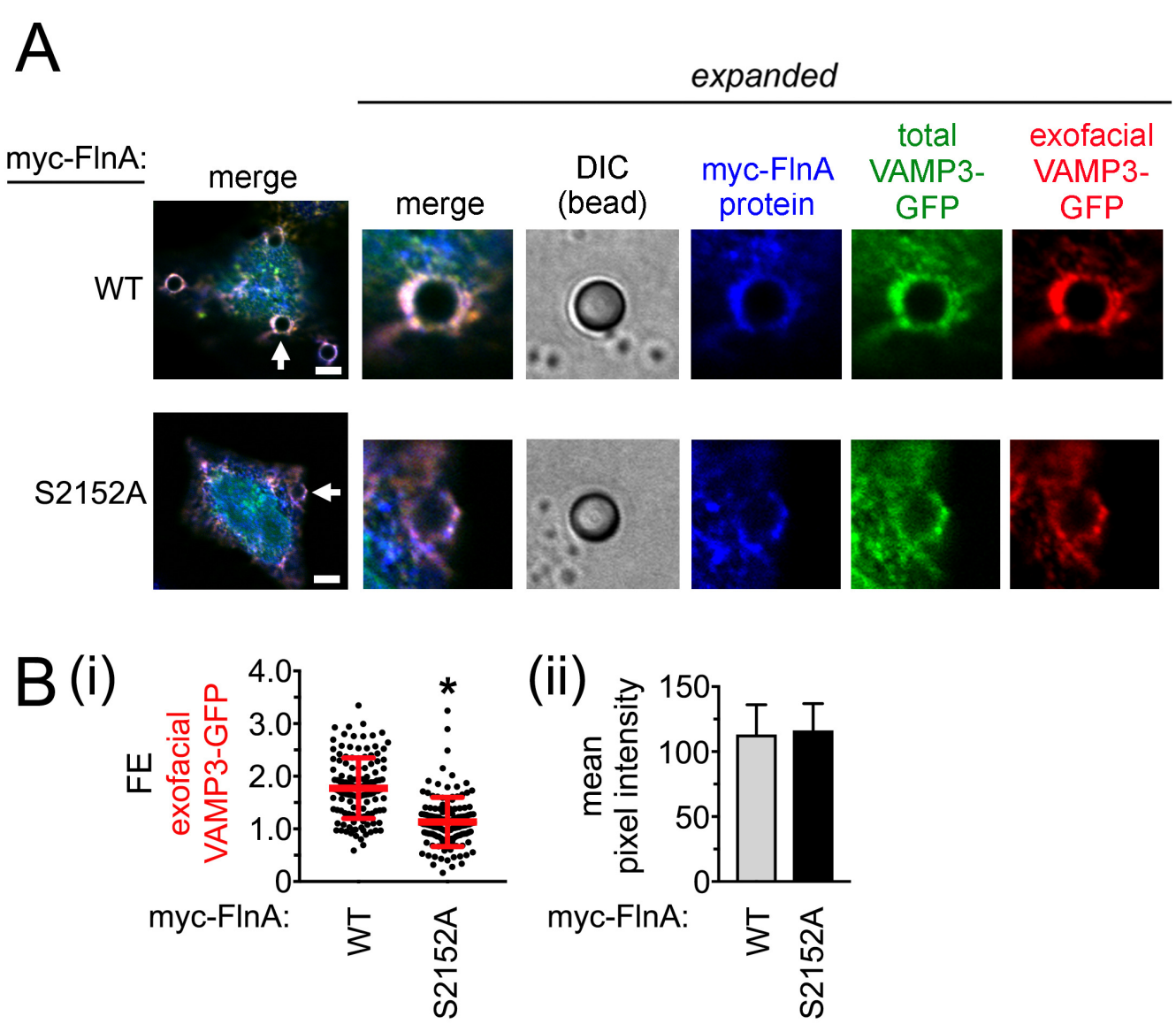

Figure 7

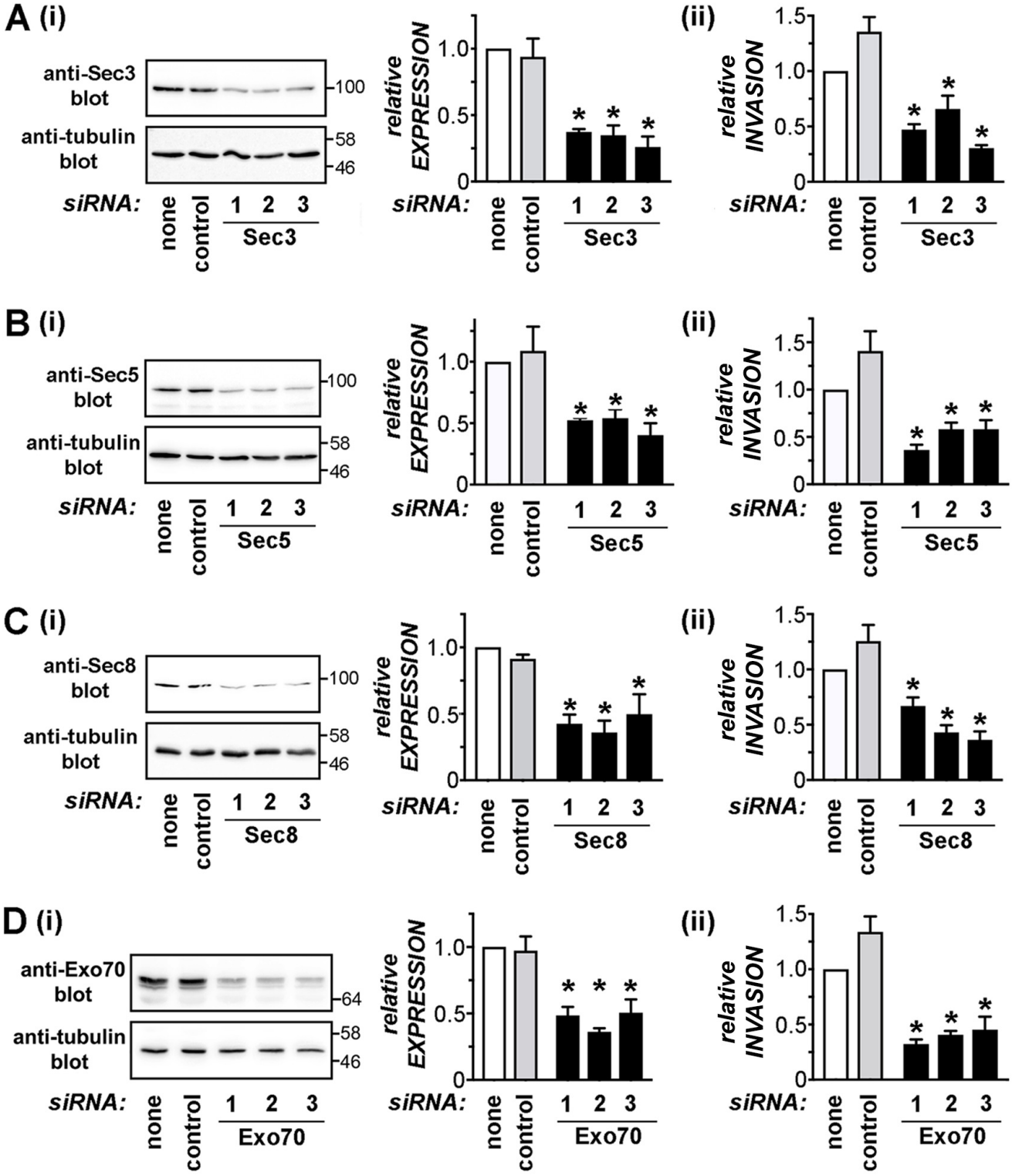

Figure 8

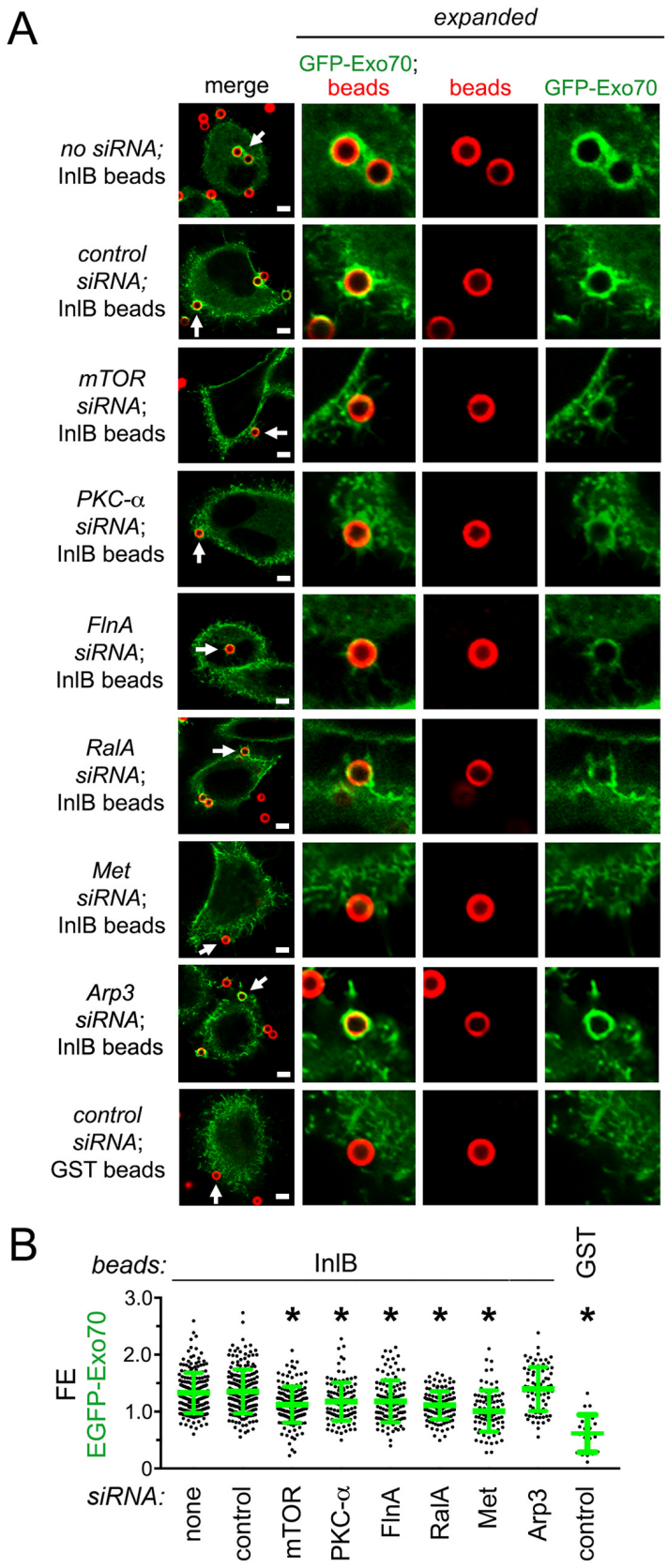

Figure 9